

Offset of coherent envelope position due to phase change on reflection

Akiko Harasaki, Joanna Schmit, and James C. Wyant

Different materials with different phase changes on reflection affect the surface-height measurement when interferometric techniques are employed for testing objects constructed of different materials that are adjacent to one another. We test the influence of this phase change on reflection when vertical scanning interferometry with a broadband source is used. We show theoretically and experimentally that the strong linear dependence of the dispersion of the phase change on reflection preserves the shape of the coherence envelope of the fringes but shifts it along the optical axis by approximately 10–40 nm for metallic surfaces. © 2001 Optical Society of America

OCIS codes: 180.3170, 120.2650, 120.3180, 120.3940.

1. Introduction

Vertical scanning interferometry (VSI)¹ is an effective way to measure surface profiles of both shallow and deep objects with nanometric resolution by means of locating the peak of the coherence envelope of the fringes for each position on the object's surface while the surface is scanned along the optical axis. The wide spectral bandwidth of the white-light source produces a short coherence length that yields high-contrast fringes at the positions where the optical path difference (OPD) is zero. However, test objects are limited to those that have the same material over the entire surface, since a different dispersion of phase change on reflection occurs for different materials, unless the height range of the object is large with respect to phase offset. The effect of this dispersion has not yet been included in the theoretical treatments of VSI techniques for surface-height measurements. Although other instruments not sensitive to phase dispersion on reflection can be used, i.e., stylus profilometer or atomic force microscope, they require a considerable amount of time for measuring large (i.e., 1 mm × 1 mm and more) sur-

face areas. Once the influence of the phase-change dispersion on VSI measurement has been determined, the correction to the measured object height can be implemented, thereby allowing for fast measurement of deep objects with regions of different materials (called here, dissimilar materials). Although there is no theoretical basis for performing VSI measurements on dissimilar materials, empirical offset corrections are sometimes used.

In this paper we propose a simple theory explaining why these traditional empirical offset treatments work, by examining the dispersion of the substrate's complex index of refraction, which influences the white-light coherence envelope of correlograms. In Section 2, the wave-number dependence of the phase change for several materials is reviewed, and then in Section 3 the change of the envelope shape or the peak location because of the dispersion of the phase change on the reflection is discussed. Once these issues have been resolved, VSI techniques are ready to be applied to dissimilar materials. Step-height measurements of metallic coatings on glass are performed for demonstration in Section 4.

2. Dispersion of the Phase Change on the Reflection

The phase change on reflection of a test surface is not constant for all wavelengths contained in a broadband light source used for VSI measurement if the extinction coefficient κ of the substrate is not zero, such as in metals and in heavily doped semiconductors. To find the influence of this dispersion, we must first know the dispersion of the phase change on reflection for a given broadband source. The phase

When this research was performed, the authors were with the Optical Sciences Center, University of Arizona, Tucson, Arizona 85721. A. Harasaki and J. Schmit (jschmit@veeco.com) were also with the Veeco Metrology Group, 2650 E. Elvira Road, Tucson, Arizona 85711. A. Harasaki is now with the 2nd Research Center, Japan Defence Agency, Tokyo, Japan.

Received 9 May 2000; revised manuscript received 9 January 2001.

0003-6935/01/132102-05\$15.00/0

© 2001 Optical Society of America

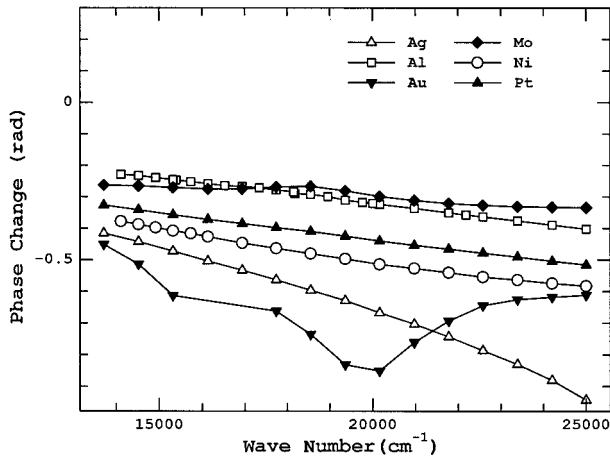


Fig. 1. Phase change on reflection of metals⁴ as a function of wave number.

change on reflection for normal incident light can be expressed as²

$$\phi_0(\nu) = \arctan \left[\frac{2\kappa(\nu)}{1 - \kappa^2(\nu) - n^2(\nu)} \right], \quad (1)$$

where n and κ are the refractive index and extinction coefficient determined theoretically or experimentally and ν is the wave number. The phase change on reflection can be also found through the use of VSI³; VSI does not require any knowledge of n and κ . Figures 1 and 2 show the phase change on reflection, which differs from π for several materials.⁴ The wave numbers, $\nu = 1/\lambda$, are chosen to correspond to the wavelength (λ) of 400–700 nm. The figures can be summarized as follows:

1. The phase change of metallic materials has dispersion as great as to 0.6 rad (35°) in the 400–700-nm wavelength region. In most cases the dependence on wave number is linear.

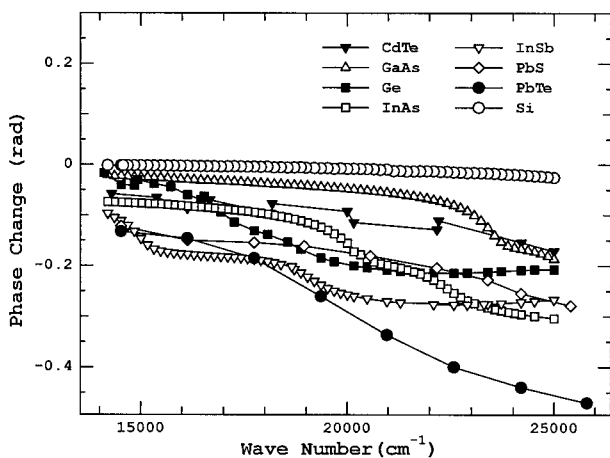


Fig. 2. Phase change on reflection of semiconductors⁴ as a function of wave number.

2. The phase change of semiconductors is more than an order of magnitude smaller than metallic materials, essentially $\phi_0(\nu) \ll 2\pi$.

3. The functional form of the phase change on the reflection of metallic materials is simpler than that of nonmetallic materials and can be approximated as a power series of wave number ν .

We conclude that the coherence envelope of the correlogram may be affected the most significantly by the dispersion of metallic materials. In addition, for metallic materials, a finite power-series expansion appears to be a good approximation to express the dispersion of phase change on reflection. For these reasons, metallic materials are the primary interest in the rest of this paper. We rewrite Eq. (1) as

$$\phi_0(\nu) = a_0 + a_1\nu + a_2\nu^2 + a_3\nu^3 + \dots \quad (2)$$

The series (2) can be truncated at the linear term, at least for metallic materials. In the case of semiconductors the dispersion of the phase change itself is very small, i.e., $a_0 + a_1\nu + a_2\nu^2 + a_3\nu^3 + \dots \ll 2\pi$. Thus in both cases the assumption of $a_2\nu^2 + a_3\nu^3 + \dots \ll 2\pi$ is valid.

3. Peak Location Shift of the Coherence Function

The modulation part of a correlogram with a flat broadband light distribution [ν_1, ν_2],

$$M(z) \propto \int_{\nu_1}^{\nu_2} \cos[2\pi\nu 2z + \phi_0(\nu)] d\nu, \quad (3)$$

is the starting point for examining the influence of the phase dispersion on the coherence envelope function. However, the same conclusion will hold for Gaussian or other types of broadband spectrum sources. Next, Eq. (2) is substituted into Eq. (3),

$$\begin{aligned} M(z) &\propto \int_{\nu_1}^{\nu_2} \cos[2\pi\nu 2z + a_0 + a_1\nu + a_2\nu^2 \\ &\quad + a_3\nu^3 + \dots] d\nu \\ &= \int_{\nu_1}^{\nu_2} \cos \left[2\pi\nu \left(2z + \frac{a_1}{2\pi} \right) + a_0 + a_2\nu^2 \right. \\ &\quad \left. + a_3\nu^3 + \dots \right] d\nu \\ &= \operatorname{Re} \left(\int_{\nu_1}^{\nu_2} \exp \left\{ -i \left[2\pi\nu \left(2z + \frac{a_1}{2\pi} \right) + a_0 \right] \right\} \right. \\ &\quad \left. \times \exp[-i(a_2\nu^2 + a_3\nu^3 + \dots)] d\nu \right). \end{aligned} \quad (4)$$

An approximation must be made for further calculation. From the analysis of phase-change dependence on wave number ν for several metallic and nonmetallic materials in Section 2, for most cases,

$$a_2\nu^2 + a_3\nu^3 + \dots \ll a_0 + a_1\nu \ll 2\pi \quad (5)$$

is a reasonable assumption. Then the second exponential term in Eq. (4) is expanded as

$$\exp[-i(a_2v^2 + a_3v^3 + \dots)] = 1 - ia_2v^2 - ia_3v^3 - \dots \quad (6)$$

Substituting this expression back into Eq. (4), we have

$$\begin{aligned} M(z) &\propto \operatorname{Re} \left(\int_{v_1}^{v_2} \exp \left\{ -i \left[2\pi v \left(2z + \frac{a_1}{2\pi} \right) + a_0 \right] \right\} \right. \\ &\quad \left. \times (1 - ia_2v^2 - ia_3v^3 - \dots) dv \right) \\ &= \operatorname{Re} \left(\int_{v_1}^{v_2} \exp \left\{ -i \left[2\pi v \left(2z + \frac{a_1}{2\pi} \right) + a_0 \right] \right\} dv \right) \\ &\quad - \operatorname{Re} \left(ia_2 \int_{v_1}^{v_2} v^2 \exp \left\{ -i \left[2\pi v \left(2z + \frac{a_1}{2\pi} \right) + a_0 \right] \right\} dv \right) \\ &\quad - \operatorname{Re} \left(ia_3 \int_{v_1}^{v_2} v^3 \exp \left\{ -i \left[2\pi v \left(2z + \frac{a_1}{2\pi} \right) + a_0 \right] \right\} dv \right) \\ &\quad - \dots \end{aligned} \quad (7)$$

The mean wave number and bandwidth can be defined as follows:

$$\bar{v} \equiv \frac{v_1 + v_2}{2}, \quad (9)$$

$$\Delta v \equiv v_2 - v_1. \quad (10)$$

After the integration is performed, the equation becomes

$$\begin{aligned} M(z) &\propto \operatorname{Re}(\exp(-ia_0)) \\ &\quad \times [\exp(-i2\pi\bar{v}\xi)\Delta v \operatorname{sinc}(\Delta v\xi)]|_{\xi=2z+a_1/2\pi} \\ &\quad + \operatorname{Re} \left(\exp(-ia_0) \frac{ia_2}{(-i2\pi)^2} \right. \\ &\quad \times \frac{d^2}{d^2\xi} [\exp(-i2\pi\bar{v}\xi)\Delta v \\ &\quad \times \operatorname{sinc}(\Delta v\xi)]|_{\xi=2z+a_1/2\pi} \\ &\quad \left. + \operatorname{Re} \left(\exp(-ia_0) \frac{ia_3}{(-i2\pi)^3} \right. \right. \\ &\quad \left. \left. \times \frac{d^3}{d^3\xi} [\exp(-i2\pi\bar{v}\xi)\Delta v \operatorname{sinc}(\Delta v\xi)]|_{\xi=2z+a_1/2\pi} \right) \right) \end{aligned}$$

$$+ \dots \quad (11)$$

The derivative operator in relation (11) must be taken care of for further calculation. When operating $d/d\xi$ once on $\exp(-i2\pi\bar{v}\xi)$, we have \bar{v} out. And operating $d/d\xi$ once on $\operatorname{sinc}(\Delta v\xi)$, we have Δv out. Since $\Delta v \ll \bar{v}$ can be assumed, the terms with higher-order Δv are dropped from the equation. Then relation (11) can be simplified as

$$\begin{aligned} M(z) &\propto \Delta v \cos(2\pi\bar{v}\xi + a_0) \operatorname{sinc}(\Delta v\xi)|_{\xi=2z+a_1/2\pi} \\ &\quad + a_2\bar{v}^2\Delta v \sin(2\pi\bar{v}\xi + a_0) \operatorname{sinc}(\Delta v\xi)|_{\xi=2z+a_1/2\pi} \\ &\quad + a_3\bar{v}^3\Delta v \sin(2\pi\bar{v}\xi + a_0) \operatorname{sinc}(\Delta v\xi)|_{\xi=2z+a_1/2\pi} \\ &\quad + \dots \\ &= \Delta v \operatorname{sinc}(\Delta v\xi) [\cos(2\pi\bar{v}\xi + a_0) + (a_2\bar{v}^2 + a_3\bar{v}^3 \\ &\quad + \dots) \sin(2\pi\bar{v}\xi + a_0)]|_{\xi=2z+a_1/2\pi}. \end{aligned} \quad (12)$$

By simple trigonometric factoring, we arrive at the final expression,

$$M(z) \propto \Delta v \operatorname{sinc}(\Delta v\xi) \cos(2\pi\bar{v}\xi + a_0 + \alpha)|_{\xi=2z+a_1/2\pi}, \quad (13)$$

and the phase α is given by

$$\alpha = \arctan(a_2\bar{v}^2 + a_3\bar{v}^3 + \dots) \approx a_2\bar{v}^2 + a_3\bar{v}^3 + \dots \quad (14)$$

The result indicates that as long as the dispersion of the phase change on reflection has a small dependence on the second and higher order of the wave number, the shape of the coherence envelope is preserved as if there were no dispersion. The linear dependence of the phase change on reflection versus wave number v shifts the location of the coherence envelope peak position by an amount of $-a_1/4\pi$. The constant term a_0 and higher-order terms α shift the fringes only underneath the coherence envelope. Suja Helen *et al.*⁵ observed that the coherence envelope peak position shifted from the zero OPD position ~ 110 nm without shape deformations in the envelope. This offset correction also can be applied to the white-light phase-shifting-interferometry-(PSI)⁶⁻⁸ type technique with a narrow-band filter source. The white-light PSI technique was developed to improve VSI height resolution to that of PSI measurement. In this case both the best contrast frame position and the phase from the best focus frame position are calculated during the vertical scanning; therefore the phase correction $a_0 + \alpha$ needs to be taken into account as well.

The height offsets resulting from both VSI and PSI techniques for several common metals are listed in Table 1. The offsets equal to $-a_1/4\pi$ are calculated from the fitted coefficients of polynomials expressed by Eq. (2) to the dispersion curves in Fig. 1. The PSI offsets are calculated with Eq. (1) at the wavelength of 600 nm, since it is the preferred wavelength for many interference microscopes during operation in PSI mode. The offsets of VSI and PSI measurements are both of the same order of magnitude and in

Table 1. Height Offsets Comparison of VSI and PSI Techniques

Metal	VSI Offset (nm)	PSI Offset ^a (nm)
Silver	36.0 ± 1.0	25.1 ± 0.2
Aluminum	13.0 ± 0.8	12.7 ± 0.1
Gold	0 ± 0.2	33.4 ± 0.5
Molybdenum	5.9 ± 0.9	13.4 ± 2.0
Nickel	15.4 ± 0.9	20.8 ± 1.8
Platinum	13.3 ± 1.0	18.1 ± 1.4

^aCalculated at the wavelength of 600 nm.

the same direction. If the metallic material is on a glass surface, the metal surface appears higher in both VSI and PSI measurements than it actually is. Usually, PSI techniques are applied to a surface with structures less than a quarter wavelength (150 nm for 600 nm illumination) in height; thus the offset that is due to the phase change on reflection might have a more serious effect in PSI than in VSI measurement.

An approximate expression of the VSI offset that is due to phase change on reflection was derived, and it can be easily verified by numerical simulations. Figure 3 shows correlograms from a glass substrate and a silver substrate after numerical performance of Eq. (3). A Gaussian light distribution from 13710 to 25000 cm⁻¹ is assumed, and the variance of the distribution is chosen such that the coherence envelope has a 1.2- μ m coherence length, as when a tungsten light bulb is used for the illumination. The peak positions were calculated with a centroid approach,⁹ and the offset was estimated to be 36 nm, which has very good agreement with the offset in Table 1 calculated by the approximate expression (13).

4. Experimental Verification and Discussion

Usually a coherence-peak-sensing technique is used to profile same-material objects, since the different offsets of coherence peak location of dissimilar materials will cause height measurement errors for

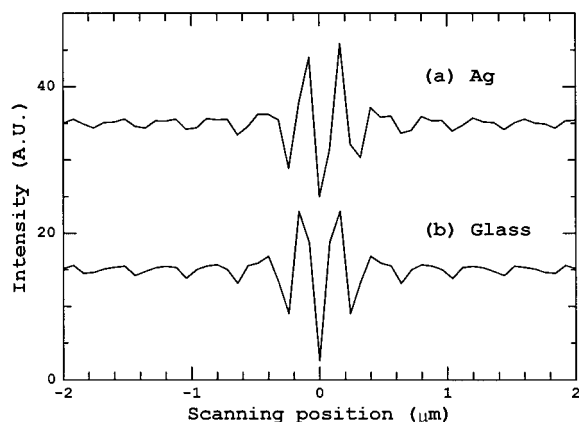


Fig. 3. Simulated correlograms, sampled every 80 nm as is typical in real measurement, from silver and glass surfaces. (a) From silver side, (b) from glass side. The offset is estimated to be 36 nm by use of the centroid approach.⁹

small height range samples. However, from the above analysis, technically, if the refractive indices and extinction coefficients of the object being tested are known, the height error might be corrected during the data processing. To verify our research, silver and aluminum steps were deposited with electron-beam evaporation (Edwards, Auto 306). The photoresist on the glass substrate was patterned prior to deposition so as to remove excess metals after deposition. This is known as the lift-off technique and is used to achieve sharp transitions. To avoid multiple reflections in the thin-film coating, which deforms the correlogram, metallic coatings were made more than 500 nm thick. The step height was measured with both VSI and PSI techniques by a Mirau interference microscope (Veeco, WYKO NT2000). Although PSI measurement gives only fractional height, we can recover the full step height by adding or subtracting $\lambda/2$ (λ is the center wavelength of the narrow-band filter used for PSI illumination), since the approximate step height is known for each sample. The average heights obtained from VSI and PSI measurement are compared at the same CCD positions. The difference is measured to be 7–10 nm for silver steps and 1–4 nm for aluminum steps, respectively. These figures correlate well with the offset difference between VSI and PSI measurement in Table 1.

Even though the refractive indices and extinction coefficients are not available to provide this nanometer height correction for every material that might be used, we believe that having an experimental correction table for different material pairs is the practical way to deal with height-error correction problems that result from the dispersion of the phase change on reflection. The regions of dissimilar materials could be assigned by the user or could be determined by an analysis of the correlogram's amplitude.

5. Conclusions

The linear dispersion of the phase change on reflection shifts the peak position of the coherence envelope function, which results in surface-height measuring errors when the object under test consists of two or more materials. Because the shift of the coherence peak is constant for a given material, the VSI technique can be applied to dissimilar materials by use of theoretical or empirical correction offsets. Metals show the largest phase dispersion on reflection, shifting the coherence peak by 10–40 nm. The offset becomes negligible when large steps of dissimilar materials are measured.

The authors thank Robert Bedford at the University of Arizona for providing the dissimilar material samples.

References

1. J. C. Wyant and J. Schmit, "Computerized interferometric measurement of surface microstructure," in *Optical Inspection and Micromasurements*, C. Gorecki, ed., Proc. SPIE **2782**, 26–37 (1996).

2. M. Born and E. Wolf, in *Principles of Optics*, 6th ed. (Pergamon, New York, 1980), p. 60.
3. J. F. Biegen, "Determination of the phase change on reflection from two-beam interference," *Opt. Lett.* **19**, 1690–1692 (1994).
4. E. D. Palik, in *Handbook of Optical Constants of Solids*, E. D. Palik, ed. (Academic, New York, 1985), pp. 275–804.
5. S. Suja Helen, M. P. Kothiyal, and R. S. Sirohi, "Phase shifting by a rotating polarizer in white-light interferometry for surface profiling," *J. Mod. Opt.* **46**, 993–1001 (1999).
6. K. G. Larkin, "Effective nonlinear algorithm for envelope detection in white light interferometry," *J. Opt. Am. A* **13**, 832–843 (1996).
7. P. Sandoz, R. Devillers, and A. Plata, "Unambiguous profilometry by fringe-order identification in white-light phase-shifting interferometry," *J. Mod. Opt.* **44**, 519–534 (1997).
8. A. Harasaki, J. Schmit, and J. C. Wyant, "Improved vertical scanning interferometry," *Appl. Opt.* **39**, 2107–2115 (2000).
9. C. Ai and E. L. Novak, "Centroid approach for estimating modulation peak in broad-bandwidth interferometry," U.S. patent 5,633,715 (27 May 1997, filed 19 May 1996).